Molecular Therapy
Original Article

Regional Hyperthermia Enhances Mesenchymal Stem Cell Recruitment to Tumor Stroma: Implications for Mesenchymal Stem Cell-Based Tumor Therapy

Mariella Tutter,[1] Christina Schug,[1] Kathrin A. Schmohl,[1] Sarah Urnauer,[1] Carolin Kitzberger,[1] Nathalie Schwenk,[1] Matteo Petrini,[2] Christian Zach,[3] Sibylle Ziegler,[3] Peter Bartenstein,[3] Wolfgang A. Weber,[4] Gabriele Multhoff,[5] Ernst Wagner,[6] Lars H. Lindner,[2] Peter J. Nelson,[1,8] and Christine Spitzweg[1,7,8]

[1]Department of Internal Medicine IV, University Hospital, LMU Munich, 81377 Munich, Germany; [2]Department of Internal Medicine III, University Hospital, LMU Munich, 81377 Munich, Germany; [3]Department of Nuclear Medicine, University Hospital, LMU Munich, 81377 Munich, Germany; [4]Department of Nuclear Medicine, Klinikum rechts der Isar der Technischen Universität München, 81675 Munich, Germany; [5]Center for Translational Cancer Research (TranslaTUM), Radiation Immuno-Oncology group, Klinikum rechts der Isar der Technischen Universität München, 81675 Munich, Germany; [6]Department of Pharmacy, Center of Drug Research, Pharmaceutical Biotechnology, LMU Munich, 81377 Munich, Germany; [7]Division of Endocrinology, Diabetes, Metabolism and Nutrition, Mayo Clinic, Rochester, MN, USA

The tropism of mesenchymal stem cells (MSCs) for tumors forms the basis for their use as delivery vehicles for the tumor-specific transport of therapeutic genes, such as the theranostic sodium iodide symporter (NIS). Hyperthermia is used as an adjuvant for various tumor therapies and has been proposed to enhance leukocyte recruitment. Here, we describe the enhanced recruitment of adoptively applied NIS-expressing MSCs to tumors in response to regional hyperthermia. Hyperthermia (41°C, 1 h) of human hepatocellular carcinoma cells (HuH7) led to transiently increased production of immunomodulatory factors. MSCs showed enhanced chemotaxis to supernatants derived from heat-treated cells in a 3D live-cell tracking assay and was validated *in vivo* in subcutaneous HuH7 mouse xenografts. Cytomegalovirus (CMV)-NIS-MSCs were applied 6–48 h after or 24–48 h before hyperthermia treatment. Using ^{123}I-scintigraphy, thermo-stimulation (41°C, 1 h) 24 h after CMV-NIS-MSC injection resulted in a significantly increased uptake of ^{123}I in heat-treated tumors compared with controls. Immunohistochemical staining and real-time PCR confirmed tumor-selective, temperature-dependent MSC migration. Therapeutic efficacy was significantly enhanced by combining CMV-NIS-MSC-mediated ^{131}I therapy with regional hyperthermia. We demonstrate here for the first time that hyperthermia can significantly boost tumoral MSC recruitment, thereby significantly enhancing therapeutic efficacy of MSC-mediated *NIS* gene therapy.

INTRODUCTION

Thermal therapy (hyperthermia) is an emerging therapeutic modality for the treatment of cancer that makes use of the diverse biological effects that occur following regionally induced heating. Hyperthermia, in contrast with fever, is defined as addition of excess heat resulting in a rise of tissue or core temperature without a regulated change in the hypothalamic set point and in absence of pyrogenic agents.[1] Although the intrinsic biologic effects of elevated temperature in cancer tissues are still not well understood, it has been well demonstrated that increasing the temperature of the tumor (39°C–42.5°C) acts as an adjuvant in multimodal cancer treatment schemes in clinical practice, such as radiotherapy and chemotherapy.[1,2] Hyperthermia is able to induce irreversible cellular DNA damage, to interfere in the DNA repair response cascades, to alter the fluidity and stability of cell membranes, and to concomitantly modify the cytoskeleton in treated cells. These physiological changes effectively sensitize tumor cells to chemotherapy or radiotherapy and can thus enhance the beneficial effects of therapeutic strategies that target DNA stability.[3] In addition, studies are currently underway using thermally labile liposomes to enhance the targeting of chemotherapy agents during regional hyperthermia.[4,5]

Regional hyperthermia has also been proposed to enhance tumor immunogenicity and can result in increased systemic tumor control by stimulating immune regulation of both the primary tumor and metastases.[6] In addition, it has been reported that heat can increase the adhesion of lymphocytes to the endothelium and thereby facilitate their infiltration.[7] The best studied phenomenon in this regard involves the enhanced trafficking of lymphocytes from draining tissues to secondary lymphatics in response to hyperthermia, primarily by the enhanced expression of chemokines, integrins, and the chemokine receptors linked to lymphoid migration (CCL21, ICAM, and CCR7; recently summarized in Skitzki et al.[8]). Mesenchymal stem

Received 5 June 2020; accepted 12 October 2020;
https://doi.org/10.1016/j.ymthe.2020.10.009.

[8]These authors contributed equally to this work.

Correspondence: Christine Spitzweg, Department of Internal Medicine IV, University Hospital, LMU Munich, Marchioninistrasse 15, 81377 Munich, Germany.
E-mail: christine.spitzweg@med.uni-muenchen.de

cells (MSCs) also show a pronounced capacity for recruitment to growing tumors; however, the exact molecular mechanisms at work in this context are not fully understood but are thought to parallel the processes underlying the recruitment of leukocytes from the peripheral circulation to inflamed tissues.[9]

MSCs are defined as multipotent progenitor cells that are capable of differentiating into multiple cell types, including osteocytes, chondrocytes, smooth muscle cells, stromal cells, and fibroblasts.[10] MSCs are characterized by a fibroblast-like morphology, a phenotypically specific cell surface marker profile, their adherence to cell culture plastic, and a high *in vitro* expansion potential.[11] *In vivo*, MSCs have the unique property of migration from the bone marrow or other tissue niches to the peripheral circulation followed by their active recruitment to sites of tissue damage and ischemia, as is generally present in solid tumors.[10] The recruitment of adoptively applied MSCs to various cancer types, such as breast cancer,[12] glioma,[13] multiple myeloma,[14] ovarian cancer,[15] colon cancer metastases,[16] hepatocellular carcinoma (HCC),[17,18] as well as pancreatic cancer,[19,20] has been demonstrated by various groups, including ours.

This general feature has made engineered versions of MSCs attractive candidates for use as shuttle vectors to efficiently deliver a therapeutic gene or agent deep into microenvironments of growing tumors.[21] The homing of MSCs is thought to depend on the combined effects of various inflammatory cytokines, chemokines, and growth factors secreted within the tumor microenvironment.[9,22] Hyperthermia has been shown to enhance the release of many of the inflammatory chemokines and cytokines shown to attract MSCs.[6,8] We hypothesized that mild regional hyperthermia could act as a means of enhancing the selective recruitment of MSCs to the tumor stroma and thus open the exciting prospect of enhancing tumor selectivity, as well as the therapeutic efficacy of MSC-mediated cancer gene therapy.

In the present report, we characterized the stimulatory effect of regional hyperthermia on recruitment of adoptively applied MSCs, engineered to express the theranostic sodium iodide symporter (*NIS*) gene under control of the cytomegalovirus (CMV) promoter, to experimental hepatocellular tumors. The HCC cell line HuH7 was chosen as the tumor model as a logical continuance of our previous work in the same model system in developing MSCs for *NIS* gene delivery. Studies using hyperthermia or external beam radiation as adjunct therapies[18,23–28] can therefore be directly compared and contrasted with regard to the efficacy of different MSC approaches. This xenograft model further effectively excludes potential confounding effects linked to the adaptive immune response.

When used as a reporter gene, *NIS* allows non-invasive monitoring of the *in vivo* biodistribution, level, and duration of functional NIS expression by ^{123}I-scintigraphy, ^{124}I-PET (positron emission tomography), or $^{99m}TcO_4$-SPECT (single-photon emission computed tomography) imaging.[16,24,25,29–31] The biology of *NIS* as a therapy gene has been widely applied in patients for over 70 years, allowing highly effective therapeutic application of ^{131}I or alternative radionuclides, such as ^{211}At or ^{188}Re.[32]

RESULTS

Effects of Hyperthermia on HCC Cell Survival Are Time and Temperature Dependent

Hyperthermic treatment led to acute cell killing only when the heat treatment was applied for an extended period of time (120 min) or at higher temperatures (42°C) (Figure S1A). In a long-term cell survival evaluation, following moderate hyperthermia (60 min at 41°C), growth of heat-treated HuH7 cells was significantly delayed *in vitro* as compared with controls as seen 5 and 7 days after heat exposure (Figure S1B).

NIS Expression and MSC Viability Are Not Sensitive to Heat Treatment for 1 h at 41°C

CMV-NIS-MSCs showed high functional NIS expression (28,114 ± 1,516 counts per minute [cpm]/A620) *in vitro* as seen in a ^{125}I uptake assay (Figure S1C), which was sensitive to the NIS-specific inhibitor perchlorate (378 ± 60 cpm/A620), demonstrating NIS dependency of the reaction (***$p < 0.001$). Thermo-stimulation caused no significant difference in ^{125}I accumulation between heated (41°C, 1 h) and non-heated CMV-NIS-MSCs (37°C, 1 h) (Figure S1D). In addition, cell viability demonstrated no significant alteration in response to mild heat treatment (Figure S1E).

Hyperthermia Alters the Inflammatory Profile of HCC Tumor Cells *In Vitro*

Diverse chemokines and cytokines have been implicated in the directed migration of MSCs.[22,33–35] We therefore sought to determine whether hyperthermic treatment could mimic inflammatory processes by stimulating the expression and secretion of a set of previously identified factors.[9,21,22] To this end, steady-state mRNA expression levels of a set of relevant factors (Table 1) were assessed in the HCC cells HuH7 after heat treatment (60 min at 41°C). The results were compared with those of untreated control cells (Figure 1). mRNA analysis indicated a substantial increase in the expression of some growth factors and chemokines after heat exposure of HuH7 cells as compared with controls (37°C). Although the tumor necrosis factor-α (TNF-α; *TNF*) (non-significant), basic fibroblast growth factor (*FGF2*), and thrombospondin-1 (TSP-1; *THBS1*) levels were found to be increased immediately (4–12 h) following hyperthermia, the chemokine *CCL15*, placental growth factor (*PGF*), and hypoxia-inducible factor 1-alpha (HIF-1α; *HIF1A*) were increased at later time points (24–48 h). 48 h after thermostimulation, the enhanced expression of many factors tested had returned to untreated control levels, while the expression of others was even reduced compared with unheated cells, such as the chemokine *CXCL8*, vascular endothelial growth factor (*VEGF*), insulin-like growth factor 1 (*IGF-1*), and *TNF*. Transforming growth factor-β (TGF-β; *TGFB1*) and *CXCL12* mRNA levels, in contrast, showed no rise but were significantly reduced by thermo-stimulation. The expression of platelet-derived growth factor-β (PDGF-β; *PDGFB*) mRNA was not significantly

Table 1. Primers for qPCR

Gene	Forward Primer (5′→3′)	Reverse Primer (5′→3′)
CXCL8	TCTGCAGCTCTGTGTGAAGG	TTCTCCACAACCCTCTGCAC
CXCL12	AGAGCCAACGTCAAGCATCT	TAGCACAGCCTGGATAGCAA
CCL15	CTGCTGCACCTCCTACATCT	CATGCAATCCTGAACTCCCG
FGF2	GGAGAAGAGCGACCCTCAC	AGCCAGGTAACGGTTAGCAC
PDGFB (PDGF-β)	TTGGCTCGTGGAAGAAGG	CGTTGGTGCGGTCTATGA
PGF	CATCCTGTGTCTCCCTGCTG	GTCTCCTCCTTTCCGGCTTC
TGFB (TGF-β)	CAGCACGTGGAGCTGTACC	AAGATAACCACTCTGGCGAGTC
VEGF	CTACCTCCACCATGCCAAGT	ATGATTCTGCCCTCCTCCTT
IGF-1	GCTGGTGGATGCTCTTCAGT	TTGAGGGGTGCGCAATACAT
TNF (TNF-α)	CAGAGGGCCTGTACCTCATC	GGAAGACCCCTCCCAGATAG
THBS1(TSP-1)	TTGTCTTTGGAACCACACCA	CTGGACAGCTCATCACAGGA
HIF1A (HIF-1α)	GCTTTAACTTTGCTGGCCCC	TTCAGCGGTGGGTAATGGAG
SLC5A5(NIS)	TGCTAAGTGGCTTCTGGGTTGT	ATGCTGGTGGATGCTGTGCTGA
		CCAATTATGTCACACCACAGA
ACTB (β-Actin)	AGAAAATCTGGCACCACACC	TAGCACAGCCTGGATAGCAA
RNA18S (r18s)	CAGCCACCCGAGATTGAGCA	TAGTAGCGACGGGCGGTGTG

altered in response to heat. No mRNA for interleukin-1 beta (*IL1B*), hepatocyte growth factor (*HGF*), epidermal growth factor (*EGF*), *CCL2*, *CCL5*, and interleukin-6 (*IL6*) was detected (data not shown).

Enzyme-linked immunosorbent assay (ELISA) was then conducted to validate effects seen at the mRNA level on protein level in supernatants of HuH7 cells (Figure 2). The chemokines CXCL12 and FGF-2 showed transiently induced protein levels in response to hyperthermic treatment (60 min at 41°C), and IL-6, PDGF-β, and IGF-1 showed the same trend without reaching significance, whereas heat resulted in reduced protein levels of CXCL8, VEGF, and TGF-β. Hyperthermic treatment was thus found to transiently mimic some aspects of an inflammatory response. To determine whether these events could elicit the directed migration of MSCs, we applied an *in vitro* migration assay.

The Heat-Stimulated Secretome of HCC Cells Enhances MSC Migration

The chemotactic behavior of CMV-NIS-MSCs in response to heat-treated (60 min at 41°C) or control HuH7 cell conditioned medium was examined using a 3D gel migration assay and time-lapse microscopy for a period of 24 h. CMV-NIS-MSCs, seeded in a collagen I matrix, showed no directed chemotaxis when subjected to supernatants derived from untreated HuH7 cells in both chambers (Figure 3A). Similarly, MSCs under the influence of a gradient between supernatants derived from untreated and heat-treated HuH7 cells 0 h (Figure 3B) and 12 h (Figure 3C) after heat treatment showed only random chemokinesis. Using supernatants collected 24 h after thermo-stimulation, however, MSCs showed directed chemotaxis toward the heat-treated supernatant (Figure 3D). This effect was even stronger with supernatants collected 48 h after hyperthermia (Figure 3E). Quantification of chemotactic parameters revealed a strong increase in forward migration index along the y axis (yFMI; Figure 3F) and mean directness (Figure 3G), a slightly increased velocity (Figure 3H), and a significant rise in the mean center of mass (yCoM) (red dots in Figures 3A, 3E) (Figure 3I) of MSCs toward supernatants from heat-treated HuH7 cells, demonstrating enhanced MSC migration toward conditioned media taken from heat-treated HuH7 cells.

Heat Treatment of Tumors Elicits an Inflammatory Response and Enhances CMV-NIS-MSC-Mediated ^{123}I Uptake *In Vivo*

As a next step, we tested whether the enhanced recruitment seen *in vitro* could be confirmed *in vivo* using a subcutaneous (s.c.) HCC (HuH7) xenograft mouse model. Quantitative analysis of tumoral radioiodine accumulation (Figure 4A) revealed a significantly increased uptake of ^{123}I in heat-treated (60 min at 41°C) as compared with non-heated tumors (tumoral iodine accumulation 1 h after ^{123}I injection of 37°C controls: 5.4 ± 0.5% injected dose [ID]/g; n = 6), with the strongest effect found in group D (8.9 ± 1.1% ID/g; n = 6), where the MSCs were injected 24 h prior to the thermo-stimulation, followed by group E (8.0 ± 1.5% ID/g; n = 6) and group C (6.5 ± 2.0% ID/g; n = 7), where MSCs were administrated 48 h before, or 6 h after, hyperthermic treatment. In contrast, when heat was applied 24 h prior to MSC injection, only a slight rise of tumoral iodine accumulation was seen in group B (6.0 ± 0.7% ID/g; n = 6) as compared with controls, and essentially control levels were seen in group A (5.9 ± 1.4% ID/g; n = 6), where regional hyperthermia was administered 48 h before the MSCs. In addition to tumoral uptake, radioiodide signals were also characteristically visible in endogenously NIS-expressing organs: thyroid, salivary glands (SGs), and

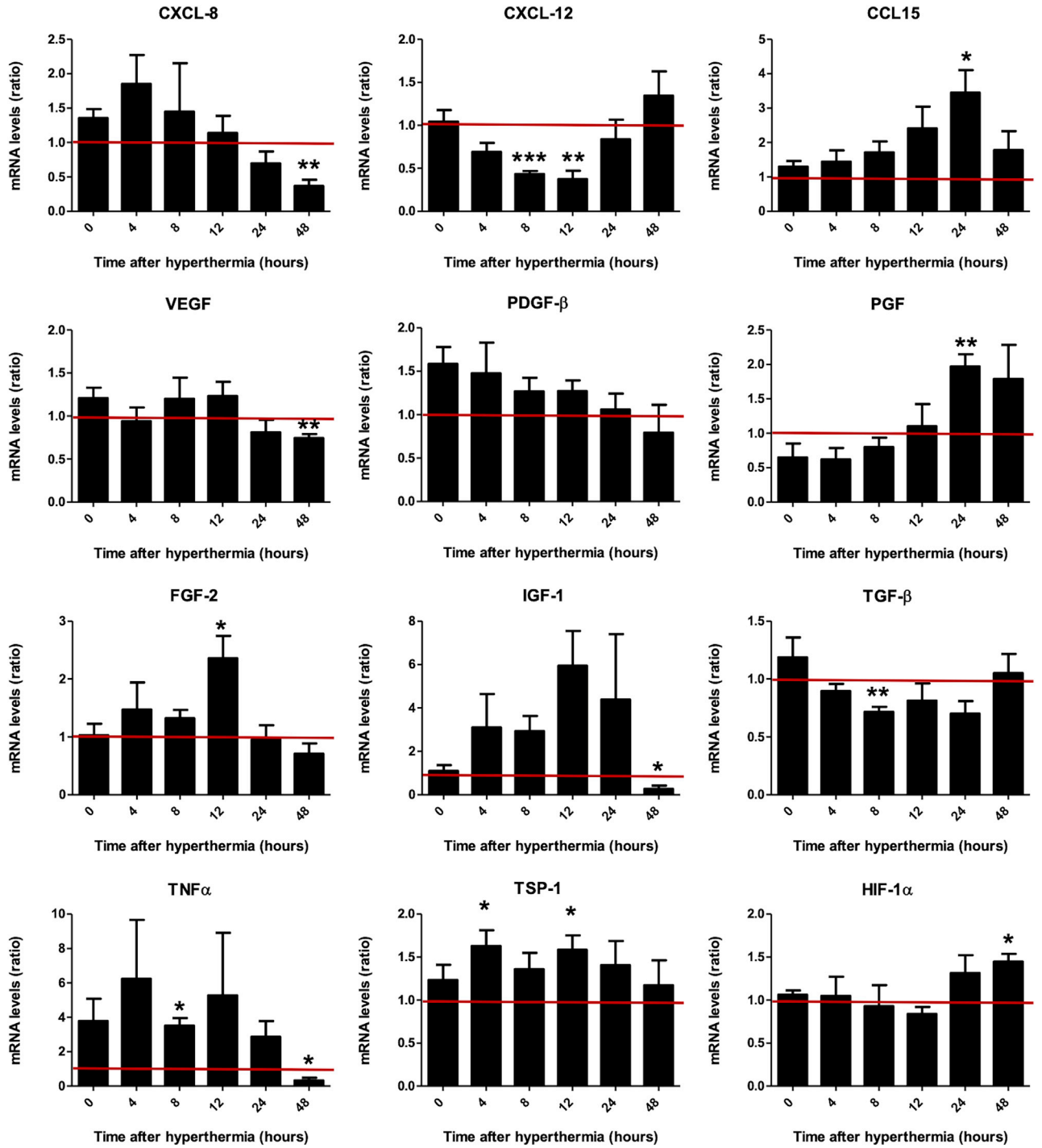

Figure 1. Chemokine and Cytokine Gene Expression Profile of HuH7 *In Vitro*

Real-time PCR analysis of mRNA extracted from heat-treated HuH7 cells 0–48 h after hyperthermia compared with non-heated HuH7 using primers listed in Table 1. Results are normalized to the internal control β-actin (*ACTB*) and expressed as mean fold change ± SEM (n = 4; two-tailed Student's t test; *p < 0.05; **p < 0.01; ***p < 0.001).

stomach, as well as in the urinary bladder, which is responsible for ^{123}I elimination. This NIS-specific iodide uptake was blocked by administration of perchlorate (Figure 4B).

Analysis of *ex vivo* steady-state mRNA levels for the *NIS* gene demonstrated significantly increased *NIS* mRNA expression in tumors heated to 41°C (1 h), as compared with controls at 37°C

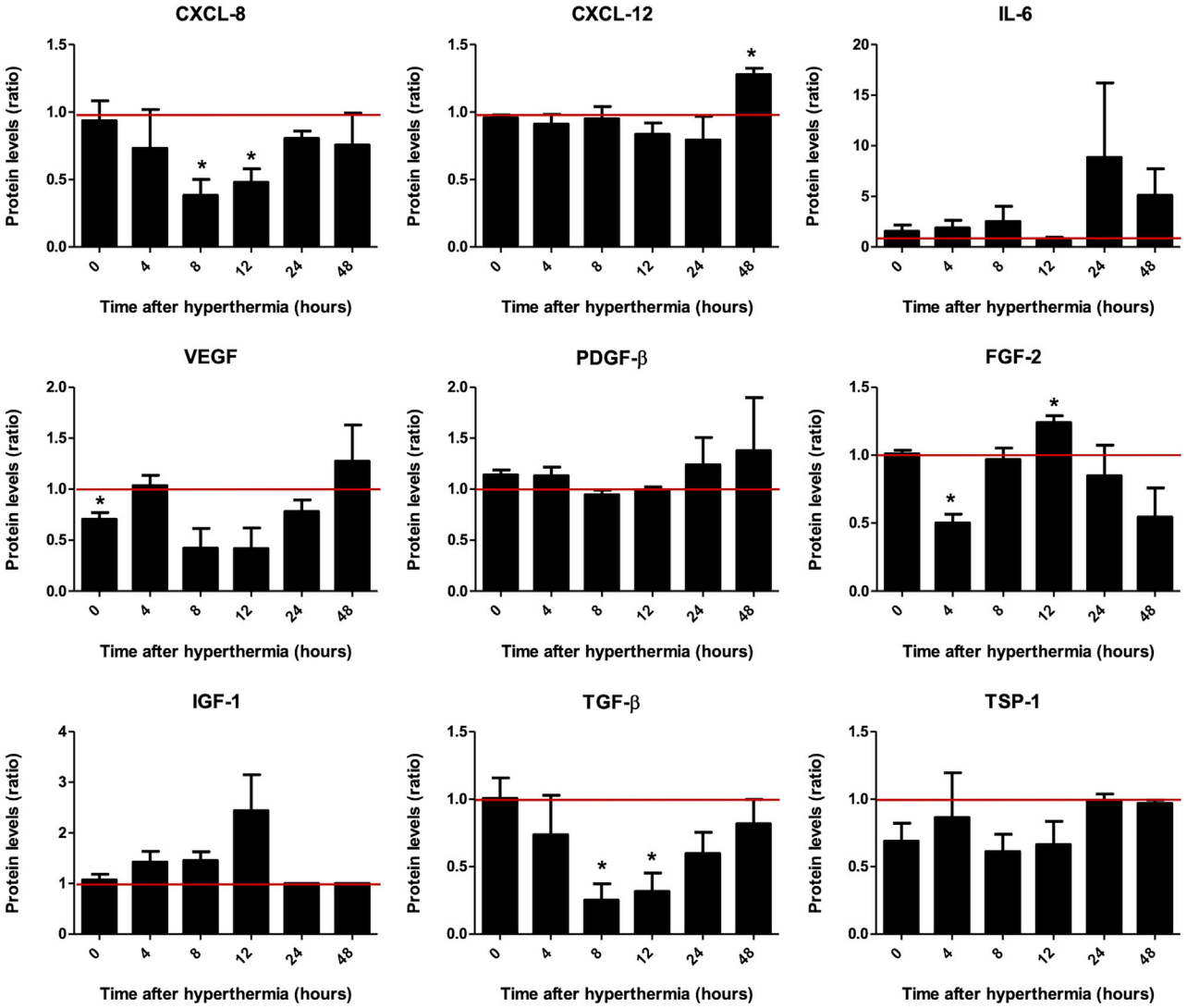

Figure 2. Chemokine and Cytokine Protein Secretion Profile of HuH7 *In Vitro*

Protein levels in culture supernatants derived from heat-treated HuH7 cells 0–48 h after hyperthermia were analyzed by ELISA. Results are presented as mean fold change ± SEM compared with non-heated control cells (n = 3; two-tailed Student's t test; *p < 0.05).

(Figure 4C). Strong NIS-specific immunoreactivity (red) was visible in the tumor stroma of heat-treated tumors, whereas controls exhibited weaker signals. No immunoreactivity was detected in non-target organs (lung, kidney, spleen, and liver), and *NIS* mRNA expression levels were below the detection limit of the qPCR (data not shown) at the time point of radioiodide injection (3 days after MSC application), confirming tumor stroma-selective MSC migration after systemic application of CMV-NIS-MSCs (Figure 4D). The *ex vivo* cytokine mRNA expression profile of heat-treated compared with unheated tumor sections (Figure 5) showed a pattern similar to the *in vitro* data, however without reaching significance, except for PDGF-β (*PDGFB*) mRNA levels that were significantly reduced after hyperthermia.

Mild Regional Hyperthermia Enhances Therapeutic Efficacy of CMV-NIS-MSC-Mediated Radioiodide Therapy

Following characterization of the optimal criteria for MSC recruitment following hyperthermia by non-invasive *in vivo* imaging, potential enhanced therapeutic efficacy of MSC-mediated *NIS* gene therapy was validated in the HuH7 xenograft mouse model using ^{131}I in combination with regional hyperthermia. The optimal application regimen of group D of the imaging series was used to verify enhanced therapeutic efficacy. Hyperthermia was applied 24 h after the systemic CMV-NIS-MSC injection, and 72 h after MSC application, therapeutic ^{131}I was administrated (Figure 6A). ^{131}I treatment combined with tumoral 41°C hyperthermia application for 60 min resulted in a significantly reduced tumor growth as compared with 37°C controls,

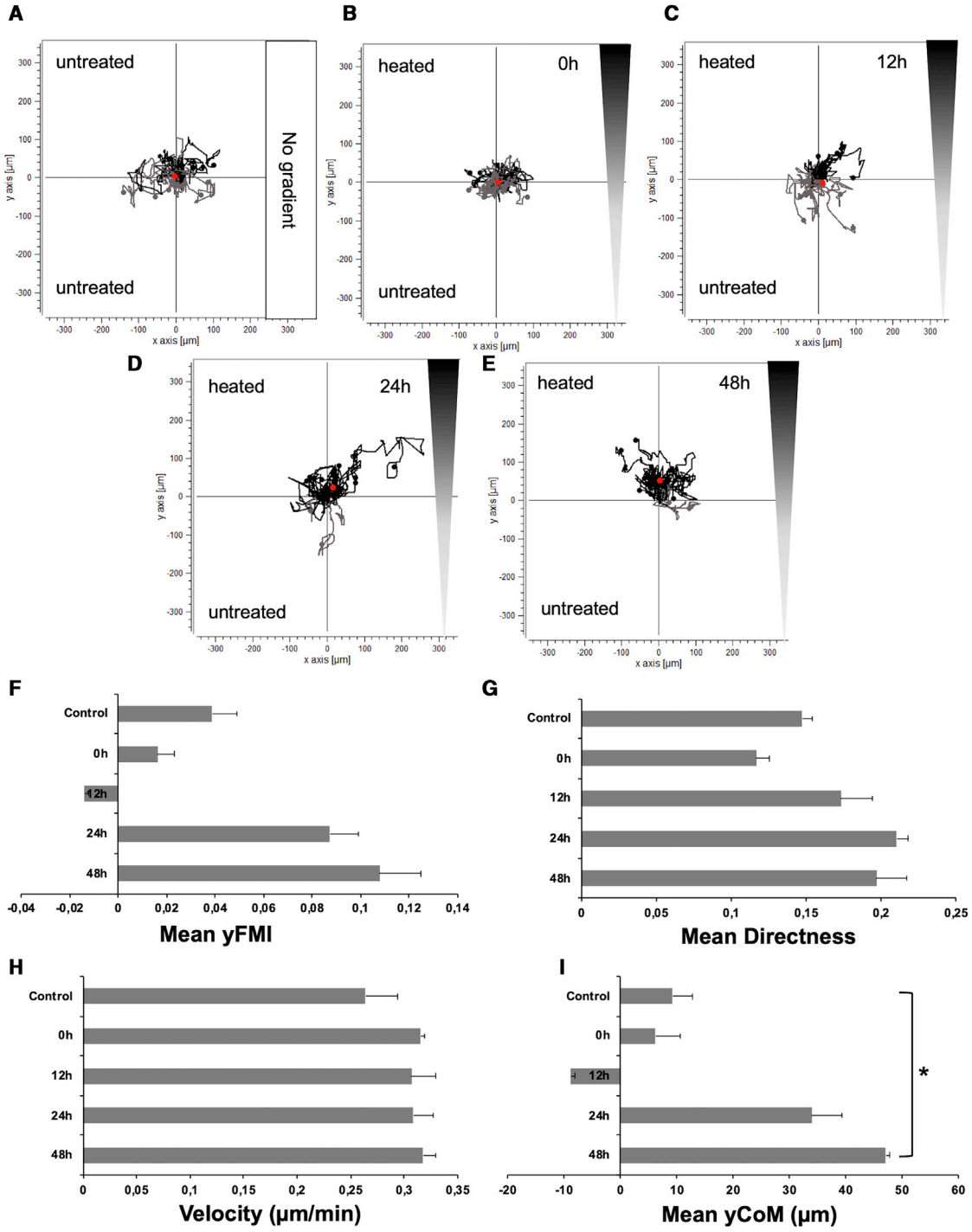

Figure 3. CMV-NIS-MSCs Migration Assay

Chemotaxis of MSCs in relation to a gradient of supernatants was tested using a live-cell tracking migration assay and monitored by time-lapse microscopy for 24 h. MSCs subjected to supernatants derived from untreated HuH7 cells in both chambers (A). Cells under the influence of a gradient between supernatants from untreated (top chamber) and thermo-stimulated HuH7 cells derived 0–48 h after hyperthermia (bottom chamber) (B–E). Quantification of chemotaxis parameters as mean forward migration index (yFMI) (F), mean directness (G), velocity (H), and the mean center of mass (yCoM; red dots in AE) (I) of MSCs toward supernatants from heat-treated compared with untreated HuH7 cells. One representative image each is shown from two independent experiments (mean ± SEM; two-tailed Student's t test; *$p < 0.05$).

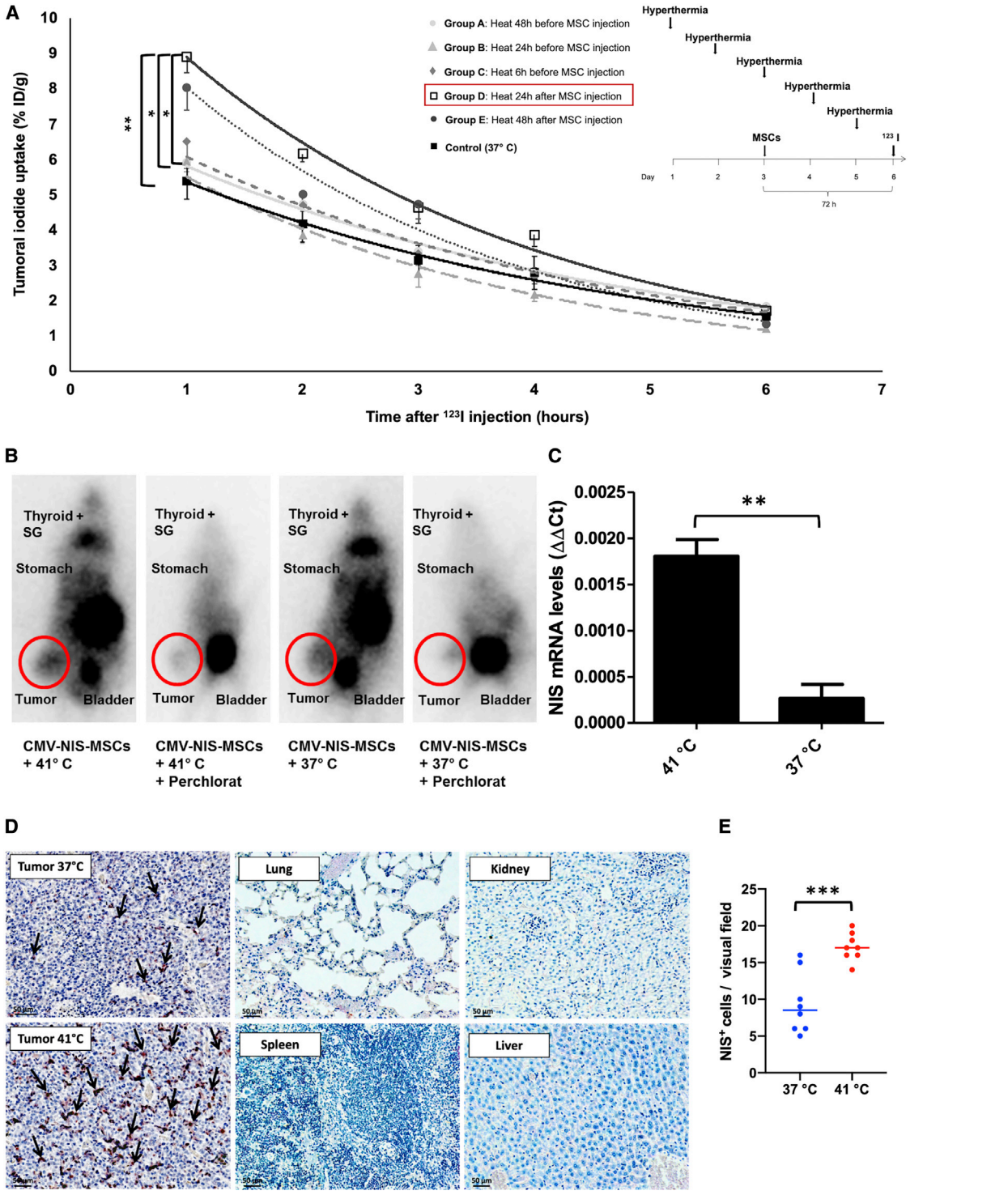

Figure 4. ^{123}I-Scintigraphy following CMV-NIS-MSC Administration

s.c. HuH7 tumor-bearing mice were injected with CMV-NIS-MSCs and subjected to hyperthermic treatment (1 h at 41°C or 37°C, as controls; n = 6) at different time points: 48 h (group A, n = 6), 24 h (group B, n = 6), 6 h (group C, n = 7) prior and 24 h (group D, n = 6, **p = 0.0055 [group D versus control], *p = 0.024 [group D versus group A], *p = 0.028 [group D versus group B], p = 0.086 [group D versus group C], p = 0.90 [group D versus group E]) and 48 h (group E, n = 6) after hyperthermia. Three days later, ^{123}I-scintigraphy was performed and tumoral iodine uptake and efflux were analyzed (A). Results are expressed as mean ± SEM, and significance was tested by ANOVA

(legend continued on next page)

and with the saline-only control group (Figure 6B), with a partial tumor remission seen in one mouse. Hyperthermia co-treatment also resulted in a prolonged survival (Figure 6C) (CMV-NIS-MSCs + 41°C + ^{131}I; n = 8) as compared with the control groups (CMV-NIS-MSCs + 37°C + ^{131}I, n = 7; saline only, n = 5). On day 26 after therapy start, all animals of the saline control had to be sacrificed because of the tumor volume reaching the allowed limit of 1,500 mm^3, whereas 85.7% of MSC + ^{131}I therapy groups were still alive, demonstrating a significantly prolonged overall survival. All mice from the 37°C controls reached endpoint criteria by day 32; at this time point 50% of the hyperthermia group was still vital. Four out of eight heat-treated mice showed a similar survival as the normothermic therapy group (approximately 30 days), whereas two of eight mice lived more than 1 week, and two of eight 100 days longer than the controls with a partial remission seen in one mouse, which had to be sacrificed on day 158 after therapy start because of a therapy-unrelated tail injury.

DISCUSSION

The tropism of MSCs for solid tumors forms the basis for their use as delivery vehicles for the tumor-specific transport of therapeutic genes, such as the theranostic *NIS*.[36] We show here that hyperthermia (41°C, 1 h) can enhance the recruitment of adoptively applied NIS engineered MSCs to the tumor stroma. This strategy supports the use of regional hyperthermia to optimize the efficacy of MSC-based *NIS* gene cancer therapy with potential for future clinical translation.

The response of cancer cells to hyperthermia is of great clinical interest. Its use as an adjuvant in multimodal treatment approaches enhances therapeutic effectiveness without increasing general toxicity. The benefit of hyperthermia in combination with radiotherapy, chemotherapy, or radiochemotherapy has been well established in various randomized clinical trials (reviewed in Rao et al.[37]). Hyperthermia shows pleiotropic effects on malignant cells and tumor tissue, including reduction of DNA repair, the production of heat shock proteins (HSPs), modulation of inflammatory cytokines, and changes in endothelial cell adhesion molecule expression. These transient changes within the tumor microenvironment are thought to help trigger an antitumor immune response.[38–40] In addition, hyperthermia is capable of increasing the amount of neutrophils, natural killer cells, and lymphocytes in the tumor microenvironment.[8] Leukocyte trafficking is a highly regulated process that may be influenced by hyperthermia at multiple stages. Hyperthermia can augment lymphocyte diapedesis across the endothelial layer, improve their adhesive properties to the endothelium, and thereby facilitate their infiltration. Chemokines, chemoattractant molecules responsive to hyperthermic stimuli, help direct leukocyte trafficking and migration.[6,8]

The exact mechanisms underlying MSC recruitment are not fully understood but are thought to parallel those seen in leukocytes. The well-characterized innate ability of MSCs to traffic to solid tumors is thought to derive from the observation that tumor stroma formation resembles a chronic, non-healing wound and MSCs are recruited to "help repair" the damaged tissue.[15,41] This general process has been adapted by many groups as a Trojan Horse-like tumor therapy approach by using engineered versions of MSCs as vehicles for the delivery of agents deep into the tumor environment.[15,21,36] This approach has now advanced to clinical trials for advanced gastrointestinal,[42] ovarian, and lung cancers (ClinicalTrials.gov: NCT02530047 and NCT03298763).

The effective homing of adoptively applied MSCs to the tumor stroma is a crucial step for successful MSC-mediated therapeutics. The priming of MSCs in culture with TNF-α or hypoxic conditions has been reported to enhance their migratory behavior *in vitro* and *in vivo*.[43,44] The functional expression of chemokine receptors, such as CXCR4, has also been shown to increase MSC homing to the bone marrow and tumors.[45,46]

Effects of MSCs on tumor progression appear to depend on the tumor type and means of MSC application used.[47,48] In our previous MSC therapy studies using the HuH7 tumor model, MSCs alone were not found to influence tumor growth.[18,28] In addition, the adoptively applied MSCs are effectively eliminated in the context of ^{131}I treatment.

In the present study, we sought to characterize the effect of regional hyperthermia on the direct recruitment of MSCs and, specifically, on events that occur within hours or days following treatment. A key question in this setting was whether regional hyperthermia could elicit processes associated with inflammation. Using a panel of genes previously associated with MSC migration, leucocyte recruitment, and inflammation,[9,21,22,33,48,49] we could show that a subset of those factors is transiently modulated at different time points following hyperthermic treatment *in vitro* (41°C for 1 h). Steady-state mRNA expression levels in HuH7 cells showed an upward trend for some genes in response to treatment starting 4 h (*CXCL8, PDGFB, TNF, THBS1*) after hyperthermia, with peak levels seen in most genes by 12–24 h (especially *CCL15, FGF2, IGF1*). Within 48 h the expression of nearly all cytokines had returned to normal or even reduced levels. By contrast, mRNA expression of *TGFB* and *CXCL12* was reduced initially in response to heat treatment. Cells respond metabolically

followed by post hoc Tukey (honestly significant difference) test. One representative image for the best performing hyperthermia treatment group and the control group, displaying besides the tumoral iodine accumulation a ^{123}I signal from the endogenously NIS expressing organs, thyroid, SGs, stomach, and the urinary bladder due to ^{123}I elimination. The competitive NIS inhibitor perchlorate was added 30 min prior to ^{123}I administration (B). mRNA isolated from frozen tumor sections was analyzed for *NIS* by real-time PCR (C) (n = 3; two-tailed Student's t test; **p = 0.0033). On paraffin-embedded tumor section, NIS-specific immunohistochemistry (red) was performed on tumors of 37°C control animals, heat-treated tumors of mice, and control organs. One representative image is shown each at 20× magnification, scale bar, 50 μm (D). Quantification of NIS staining on tumor sections (dots represent counts in a single visual field, lines represent the median) (E).

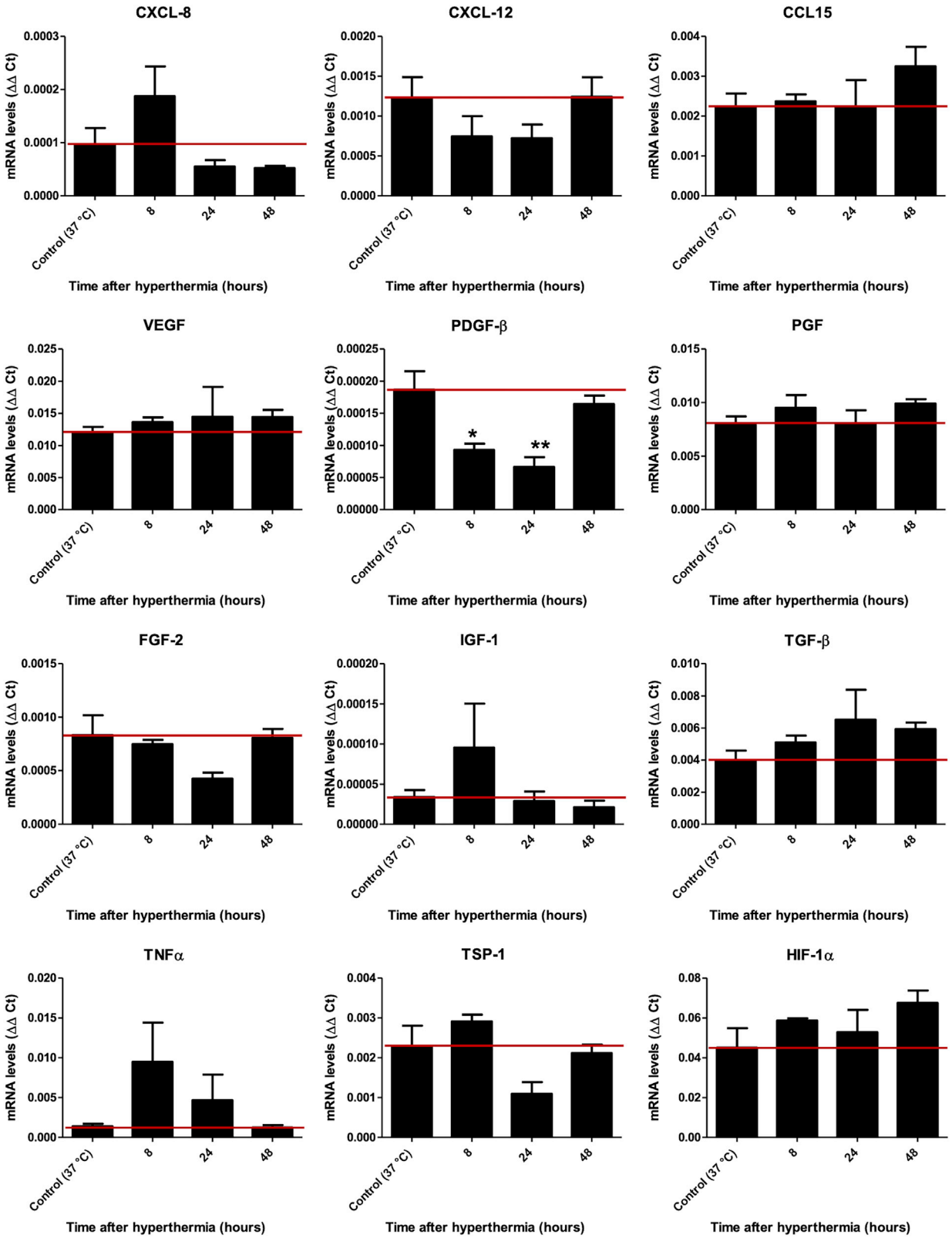

(legend on next page)

when subjected to a heat challenge. They upregulate HSPs and other cell-protective proteins, while reducing the steady-state levels of genes not involved in the heat response.[2] Subsequent mRNA analysis of heat-treated tumor sections *ex vivo* presented a similar trend of time-dependent cytokine secretion as seen *in vitro*, thereby corroborating the upregulation of immunomodulatory factors potentially enhancing MSC migration *ex vivo*. These general effects were further validated in a 3D migration model that showed enhanced migration toward conditioned media taken from heat-treated HuH7 cells.

The effects of the heat treatment protocol (41°C for 1 h) on cell viability *in vitro* were characterized, and a slight reduction in HuH7 cell viability was observed. The cell viability of MSCs was not affected by mild heat treatment, and no significant difference in ^{125}I accumulation was seen between heated (41°C) and non-heated CMV-NIS-MSCs (37°C). This confirms the previous observation that normal tissues are generally not damaged during hyperthermia,[50] whereas tumors are more sensitive to hyperthermia.[51] However, effects of hyperthermia on MSCs have been reported in previous studies. Periodic hyperthermic treatment of bone marrow MSCs was found to enhance their differentiation into osteoblasts and accelerated maturity.[52] Alekseenko et al.[53] demonstrated that mild heat treatment of menstrual blood MSCs did not affect the viability of MSCs *in vitro*. Only cells challenged with "sublethal" heating (45°C for 30 min) presented signs of stress-induced premature senescence, but surviving MSCs retained the properties of parental cells.[53] Rühle et al.[54] observed that after hyperthermia, MSCs remain viable and do not change their surface marker expression profile or their motility in response to hyperthermia.

The enhanced recruitment effects seen in the *in vitro* experiments were validated *in vivo*. A promising candidate therapy gene for the next generation of clinical applications of MSC-mediated cancer therapy is the *NIS* transgene. *NIS* as a well-characterized theranostic gene that allows detailed non-invasive *in vivo* tracking of MSCs by ^{123}I-scintigraphy or ^{124}I-PET imaging, as well as highly effective therapeutic application of radionuclides (^{131}I, ^{188}Re).[31] We and others have demonstrated MSC-mediated transfer of therapeutic transgenes to diverse cancer entities, including HCC,[23,24] glioma,[13] breast cancer,[55] prostate cancer,[56,57] colon cancer metastases,[16] multiple myeloma,[58] and pancreatic ductal adenocarcinoma.[19,20] In our studies using the *NIS* theranostic gene, we have found that MSC injections followed by the therapeutic administration of ^{131}I have led to significantly reduced tumor growth with a prolonged survival of animals in multiple experimental tumor settings.[18,24,26,59]

In the present study, a single systemic injection of CMV-NIS-MSCs combined with thermo-stimulation at 41°C showed that hyperthermia enhances the selective migration of MSCs into the tumor stroma of murine s.c. HCC (HuH7) xenografts. Testing the application of heat at different time points 48, 24, and 6 h before and 24 and 48 h after MSC injection, we observed the highest tumoral iodine uptake when injecting MSCs 24 h prior to hyperthermia (group D). After intravenous injection, MSCs are initially trapped in the microcapillaries of the lungs and start to migrate from the lungs to other organs, such as the liver, spleen, or kidneys, or, if present, to a tumor only after 24 h.[60–62] This effect may help explain our observation that the highest recruitment was seen after applying heat 24 h after MSC injection, which may represent optimized timing of the transiently enhanced tumoral cytokine secretion following hyperthermia with the egress of the adoptively transferred cells from the lungs.

The optimal regional hyperthermia recruitment protocol identified by non-invasive imaging using ^{123}I-scintigraphy was then further tested and validated in the context of *NIS* gene-based ^{131}I-therapy. Animals treated with MSCs, hyperthermia, and ^{131}I showed significantly reduced tumor growth and a prolonged survival compared with the normothermic group and with the saline control group, demonstrating a significantly improved efficacy of MSC-mediated *NIS* gene therapy. In a parallel study by our group using the same HuH7 tumor model, no effect of hyperthermia was observed on either tumor growth or survival when MSCs were applied without ^{131}I (MSCs + 41°C + NaCl versus MSCs + 37°C + NaCl) even after up to three rounds of hyperthermic therapy.[28] For this reason, in the present study we do not believe that hyperthermia-induced tumor cell death is responsible for the therapy effect observed. In addition, past studies with the same model have shown that treatment with MSCs without ^{131}I (MSCs + NaCl) did not influence tumor growth.[18] The tumoral therapy response here showed signs of a late divergence in tumor growth and survival curves, a phenomenon that has been described in immune therapy trials, as well in a phase III trial of neoadjuvant chemotherapy plus regional hyperthermia.[63,64] In our *in vivo* therapy, overall, we observed a heterogeneous response to the therapy, with four out of eight hyperthermia-treated mice showing a clear therapeutic effect from significant reduction of tumor growth to a partial remission. Heterogeneous response rates have also been seen in clinical hyperthermia trials, such as in the recent EORTC 62961-ESHO 95 phase III trial on neoadjuvant chemotherapy alone or with regional hyperthermia for localized high-risk soft tissue sarcoma.[63] We believe that a main reason for the heterogeneous response may be our experimental setup for hyperthermia using a conventional water bath with its limitations in establishing and monitoring stable and homogeneous intratumoral temperatures. Several trials have demonstrated a strong correlation between intratumoral temperatures and response to treatment.[65] Recent technical improvements in the sources used to apply and measure heat have expanded

Figure 5. Chemokine and Cytokine Secretion Profile of HuH7 *In Vivo*

mRNA was isolated from frozen tumor sections from heat-treated tumors 8, 24, and 48 h later, including 8 h ^{123}I imaging (each n = 4) and controls (n = 4), and expression levels of different chemokines and cytokines were evaluated by real-time PCR. Results are normalized to the internal control (average of *ACTB*, *r18s*, and *UBC*) and expressed as mean ± SEM (two-tailed Student's t test; *$p < 0.05$; **$p < 0.01$).

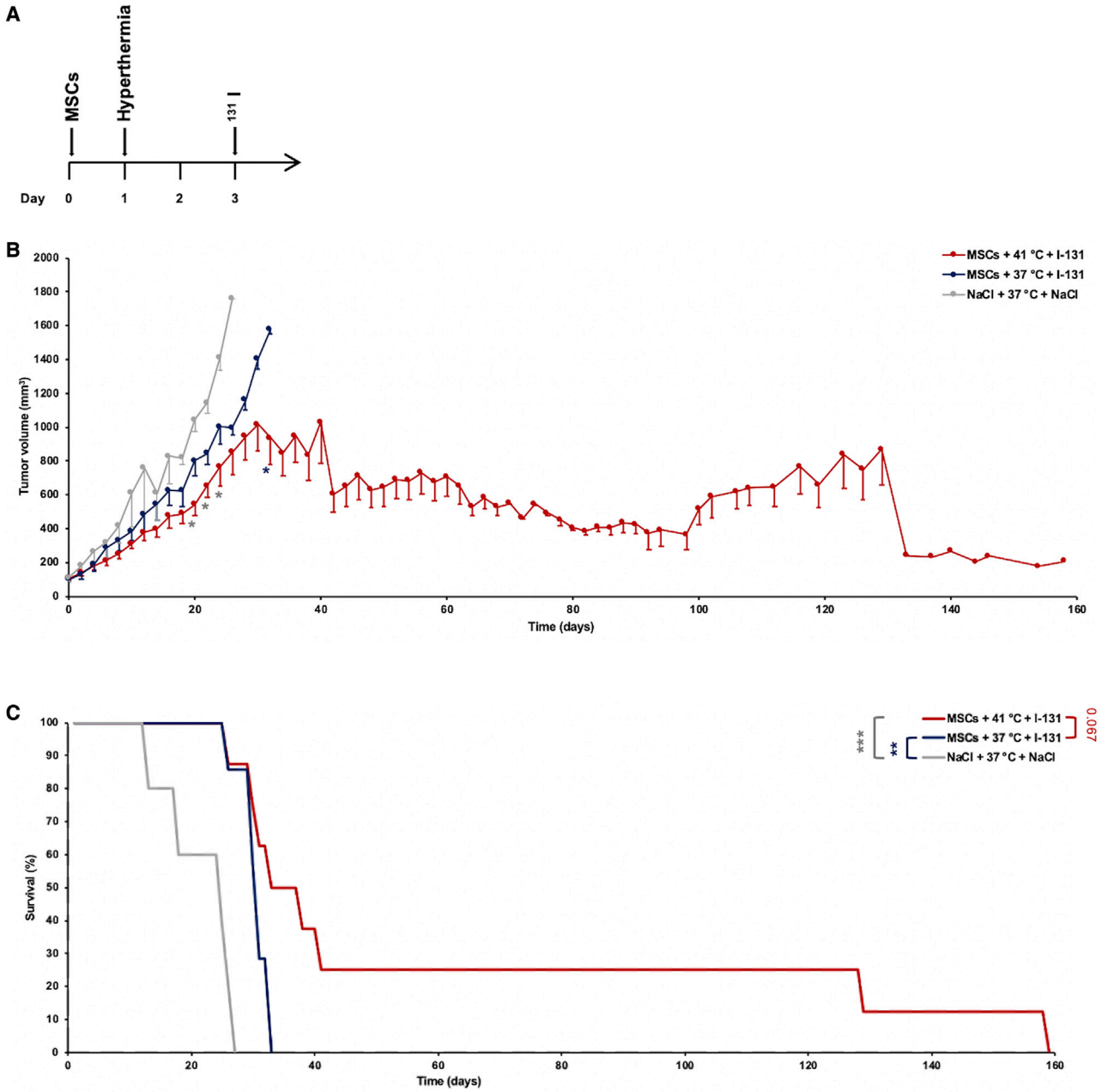

Figure 6. *In Vivo* ^{131}I Therapy Study

In a s.c. HuH7 xenograft mouse model, the best treatment scheme identified in the imaging study was adapted for a therapy study using ^{131}I (A). Tumor growth (B) and survival (C) were monitored for the treatment with CMV-NIS-MSCs, regional hyperthermia, and ^{131}I (MSCs + 41°C + ^{131}I; n = 8; red line), compared with the normothermic control group (MSCs + 37°C + ^{131}I; n = 7; blue line) and the saline only group (NaCl + 37°C + NaCl; n = 5; gray line). Results are expressed as mean ± SEM (one-way ANOVA for tumor growth and log-rank test for Kaplan-Meier survival plots; *$p < 0.05$; **$p < 0.01$; ***$p < 0.001$).

the clinical use of hyperthermia. In this regard, hybrid magnetic resonance-guided high-intensity focused ultrasound has been adapted for tumor hyperthermia therapy that allows a highly focused heating of the region with real-time temperature mapping and energy deposition.[66]

The results outlined here show that the natural tropism of exogenously applied MSCs for solid tumors can be transiently enhanced by the application of regional hyperthermia. Because the directed recruitment of adaptively applied MSCs involves a complex interplay of various factors (inflammatory cytokines and chemokines) and

cellular events (rolling across the endothelium, firm adhesion, diapedesis, etc.), the identification of the central players mediating the enhanced effects seen in the context of regional hyperthermia will require extensive future studies.

Using *NIS* in its function as reporter gene, we were able to determine the optimal timing of hyperthermia treatment in the course of MSC application by non-invasive imaging that ultimately resulted in a significant therapeutic effect of CMV-NIS-MSC-based ^{131}I therapy in liver cancer xenografts. These data open the promising prospect of using hyperthermia to enhance the effectiveness of MSC-mediated cancer gene therapy for future clinical application and of potential implementation of this strategy in other MSC-based therapy contexts such as regenerative medicine.

MATERIALS AND METHODS

Cell Culture and *In Vitro* Studies

SV40 large T antigen-immortalized human bone marrow-derived MSCs were stably transfected with *NIS* driven by the CMV promoter (CMV-NIS-MSCs) as described previously.[18] The MSC cell line (CMV-NIS-MSCs) was grown in RPMI-1640 culture medium (Sigma-Aldrich, St. Louis, MO, USA) and supplemented with 10% (v/v) fetal bovine serum (FBS; FBS Superior; Biochrom/Merck Millipore, Berlin, Germany), 100 U/mL penicillin and 100 µg/mL streptomycin (P/S; Sigma-Aldrich), and 1% geneticin (G-418; Invitrogen, St. Louis, CA, USA). The human HCC cell line HuH7 (JCRB0403; Japanese Collection of Research Bioresources Cell Bank, Osaka, Japan) was cultured in Dulbecco's modified Eagle's medium (DMEM; 1 g/L glucose; Sigma-Aldrich) enriched with 10% (v/v) FBS and 1% P/S. Both cell lines were kept in an incubator at 37°C, 5% (v/v) CO_2 atmosphere, and 95% relative humidity.

For *in vitro* heat treatment, cell culture dishes were sealed with parafilm and submerged in a circulating water bath for 30, 60, or 120 min at 40°C, 41°C, or 42°C, followed by a recovery time in an incubator at 37°C (5% CO_2, 95% humidity) for 0, 1, 2, 5, or 7 days based on previously established methods.[4,28] In a series of unpublished, preliminary heat treatment experiments, the water bath system was calibrated using exact temperature measurements to reach the desired temperature inside of our plastic cell culture dishes. For all of the following experiments, the same standard heat treatment protocol (41°C + 60 min) was chosen, because this temperature is clinically most relevant.

For the preparation of HuH7 supernatants, 1×10^6 HuH7 cells were seeded in a 100 mm^3 cell culture dish, and 12 h before thermo-stimulation full-growth medium was replaced by serum-free DMEM. Supernatants from heat-treated and non-treated cells were collected 0, 4, 8, 12, 24, and 48 h after heat treatment and immediately stored at −80°C.

Cell Viability Assay

Cell viability was determined using a commercially available thiazolyl blue tetrazolium blue (MTT) reagent (Sigma Aldrich) for 2 h at 37°C. The absorbance of the resulting formazan product was measured after incubation with 10% (v/v) dimethylsulfoxide (DMSO; Sigma Aldrich) in isopropanol (Carl Roth, Karlsruhe, Germany) at a wavelength of 620 nm, using a Sunrise microplate absorbance reader and the Magellan software (Tecan, Männedorf, Switzerland).

^{125}I Uptake Assay

Functional NIS expression of CMV-NIS-MSCs was determined *in vitro* using a ^{125}I uptake assay at steady-state conditions as described previously.[28] In brief, 0.1 µCi Na^{125}I/mL (PerkinElmer, Waltham, MA, USA), Hank's balanced salt solution (GIBCO/Life Technologies, Carlsbad, CA, USA), 10 mM 4-(2-hydroxyethyl)-1-piperazineethanesulfonic acid (HEPES; Sigma) (pH 7.3), and 10 µM NaI was added to the wells, and the cells were incubated for 45 min at 37°C. To demonstrate NIS specificity of iodide uptake, we added the NIS-specific inhibitor $KClO_4$ (100 mM; Merck Millipore, Burlington, MA, USA) to control wells. After washing, cells were lysed in 1N NaOH (Carl Roth, Karlsruhe, Germany) for 15 min, and captured ^{125}I was investigated by γ-counting (Beckman Coulter, Krefeld, Germany). Results were normalized to cell survival and expressed as cpm/A620.

Quantitative Real-Time PCR and ELISA

HuH7 RNA was isolated from heat-treated and control cells 0, 4, 8, 12, 24, and 48 h after hyperthermia using the RNeasy Mini Kit with QIAshredder (QIAGEN, Venlo, the Netherlands) according to the manufacturer's recommendations. Reverse transcriptase reaction was performed using Superscript III reverse transcriptase (Invitrogen, Carlsbad, CA, USA), and the quantitative real-time PCR was run in a Mastercycler ep gradient S PCR cycler (Eppendorf, Hamburg, Germany) or a LightCycler 96 System (Roche, Basel, Switzerland) using the primers listed in Table 1. ΔΔ−Ct values were normalized to the internal control (β-actin; *ACTB*), and results were expressed as fold change relative to un-heated controls.

An ELISA of supernatants derived from HuH7 cells 0–48 h after heat exposure (41°C or 37°C, as controls) was performed using the respective DuoSet ELISA Kit (R&D Systems, Abington, UK) according to the manufacturer's recommendations. Relative protein levels were calculated as fold change relative to controls.

3D Migration Assay

Chemotaxis of MSCs, seeded in collagen I (0.3×10^6 cells/mL), in relation to a gradient of unheated and heat-treated HuH7 supernatants, was tested in a live-cell tracking migration assay using the µ-slide Chemotaxis^{3D} system (ibidi, Planegg, Germany) and monitored by time-lapse microscopy (Leica Microsystems, Wetzlar, Germany) for 24 h as previously described.[26] Every 15 min a picture was taken, using a Jenoptik ProgRes charge-coupled device (CCD) camera (Jenoptik, Jena, Germany) and an automatic xy-stage (Prior Scientific, Jena, Germany), controlled by the open access software ImageJ (NIH, Bethesda, MD, USA) using the µManager plug-in. The ImageJ Manual Tracking plug-in (Fabrice Cordelières, Orsay, France) was used to track 20 randomly selected cells, and the

Chemotaxis and Migration Tool plug-in (ibidi) was used for analysis of migration. The following parameters were evaluated to quantify cell migration: the yFMI is obtained by dividing the displacement of each cell along the y axis by its total path length and represents a measure of the migration potency of the cells toward one supernatant in the direction of the gradient; the yCoM (μm) expresses the median endpoint of the single cells and direction of migration; the velocity (μm/min) of the migrating cells is determined; directness (D) is measured with D = 1 representing a straight-line migration; and the Rayleigh value derives from a statistical test for circular distribution of points ($p < 0.05$ statistically significant).

Establishment of s.c. HuH7 Xenografts

Establishment of s.c. HuH7 xenograft mouse model in female CD1 nu/nu mice (Charles River, Sulzfeld, Germany), which were maintained under specific pathogen-free conditions with *ad libitum* access to mouse chow and water, was performed as described previously.[18] In brief, mice were s.c. injected with 5×10^6 HuH7 cells suspended in 100 μL phosphate-buffered saline (PBS; Sigma Aldrich) into the right flank region. s.c. tumors were measured using a caliper, and volumes were calculated using the following equation: length × weight × height × 0.52. 10 days prior to iodine application, 5 mg/mL L-thyroxine (L-T4; Sigma-Aldrich) was added to drinking water to reduce thyroidal radioiodine accumulation. All animal experiments were approved by the regional governmental commission for animals (Regierung von Oberbayern, Munich, Germany). Potential hyperthermic effects on adaptive anti-tumor immunity could be excluded based on the mouse model used (CD1 nu/nu mice).

In Vivo Regional Hyperthermia

For regional hyperthermic treatment, mice were anesthetized by inhalation of isoflurane/oxygen anesthesia and placed on top of a water bath at 41°C or, as control, at 37°C for 1 h. The water bath was covered with a plastic plate specifically designed to allow only the tumor-bearing leg to be submerged into the water, through small holes in the plastic cover. Body temperature was monitored using a rectal thermometer (Homeothermic Blanket Systems with Flexible Probe; Harvard Apparatus, MA, USA).

In a series of pilot heat treatment experiments, to confirm stable and sufficient heat delivery into the tumor, a thermo probe was placed intratumorally, and tumor temperature was monitored over the entire treatment time (60 min) to establish our treatment parameters (Figure S2). A rapid, stable, and reliable tumoral temperature delivery was confirmed (Figure S2A), while body temperature of mice stayed within physiological levels (Figure S2B). These preliminary studies allowed us to conduct the following experiments without a tumoral probe, which would distort our results because the wound caused by the probe would artificially enhance MSC recruitment.

^{123}I-Scintigraphy after *NIS* Gene Transfer

When the tumors reached a volume of 500–800 mm^3, a single systemic injection of 0.5×10^6 CMV-NIS-MSCs into the tail vein was applied to HuH7 tumor-bearing mice, and hyperthermia was locally applied either 48 h (n = 6), 24 h (n = 6), or 6 h (n = 7) before or 24 h (n = 6) or 48 h (n = 6) after MSC injection. To reduce the number of animals, we conducted the control normothermic group (37°C; n = 6) in the same way as the best hyperthermic group (group D; MSCs 24 h before heat treatment). Seventy-two hours after MSC administration, mice received 18.5 MBq ^{123}I (GE Healthcare Buchler, Braunschweig, Germany) intraperitoneally (i.p.), and iodide biodistribution was measured by serial scanning (1–6 h) on a gamma camera (e.cam; Siemens, Munich, Germany) using a low-energy, high-resolution collimator. As control of NIS-specific iodide accumulation, the NIS inhibitor perchlorate (Merck, Darmstadt, Germany) was injected 30 min prior to ^{123}I injection. Regions of interest (ROIs) were analyzed by HERMES GOLD (Hermes Medical Solutions, Stockholm, Sweden) software, and tumoral iodide accumulation was expressed as % of the ID per gram tumor (% ID/g).

Ex Vivo Analysis

Immunohistochemical staining of paraffin-embedded tumor sections and control organs was performed using a NIS-specific antibody (dilution 1:500; Merck Millipore) as described previously.[67] Tumor and organ samples taken 8, 24, and 48 h after heat treatment (including 8 h ^{123}I-scintigraphy) were analyzed by real-time PCR. ΔΔ−Ct values were normalized to the internal control (the average of *ACTB*, *UBC*, and *r18s*).

^{131}I-Therapy Study

Approximately 10 days after s.c. HuH7 cell injection, when tumors had reached a size of 5 mm in diameter, the drinking water was supplemented with 5 mg/mL L-T4 (Sigma Aldrich), and the mice received a low-iodine diet (ssniff Spezialdiäten, Soest, Germany) to potentially enhance tumoral iodide accumulation and to reduce thyroidal iodide uptake. At a tumor volume of around 100 mm^3, the mice received a single systemic injection of CMV-NIS-MSCs via the tail vein, followed by hyperthermic treatment (41°C or 37°C for 1 h) 24 h later. 2 days after hyperthermia, 55.5 MBq ^{131}I was applied i.p. (CMV-NIS-MSCs + 41°C + ^{131}I, n = 8; CMV-NIS-MSCs + 37°C + ^{131}I, n = 7). As the control group, MSCs and ^{131}I were replaced by saline, and mice were treated with 37°C (NaCl + 37°C + NaCl, n = 5). Mice were sacrificed based on tumor growth (tumor volume exceeded 1,500 mm^3) and animal care protocols.

Statistical Analysis

All *in vitro* experiments were performed at least three times, and values are expressed as mean ± SEM. Rayleigh value was used for analysis of MSC migration. Statistical significance was tested by two-tailed Student's t test or by ANOVA with post hoc Tukey (honestly significant difference) test for multiple comparisons. Survival was plotted by Kaplan-Meier survival plots and analyzed by log-rank test. p values < 0.05 were considered significant (*$p < 0.05$; **$p < 0.01$; ***$p < 0.001$).

SUPPLEMENTAL INFORMATION

Supplemental Information can be found online at https://doi.org/10.1016/j.ymthe.2020.10.009.

AUTHOR CONTRIBUTIONS

Conceptualization: M.T., K.A.S., L.H.L., P.J.N., C.S.; Methodology: M.T., M.P., L.H.L., P.J.N, C.S.; Investigation: M.T., C.S., S.U., C.K., N.S.; Formal Analysis: M.T., C.Z.; Resources: S.Z., P.B., W.W., G.M.; Writing – Original Manuscript: M.T.; Writing – Review & Editing: K.A.S., G.M., E.W., L.H.L., P.J.N., C.S.; Funding Acquisition: P.J.N. and C.S.; Supervision: E.W., L.H.L., P.J.N., C.S.

CONFLICTS OF INTEREST

The authors declare no competing interests.

ACKNOWLEDGMENTS

We are grateful to Dr. Barbara von Ungern-Sternberg, Rosel Oos, and Dr. Markus Strigl (Department of Nuclear Medicine, University Hospital, LMU Munich, Munich, Germany), and Jakob Allmann (Department of Nuclear Medicine, Klinikum rechts der Isar der Technischen Universität München, Munich, Germany) for their support with imaging and therapy studies. The authors thank Prof. Doris Mayr (Department of Pathology, University Hospital, LMU Munich, Munich, Germany) for preparation of paraffin-embedded slides. We also thank our team members Dr. Viktoria Köhler, Yang Han, and Rebbeka Spellerberg for their help with the revision of the manuscript. This work was supported by the Deutsche Forschungsgemeinschaft, Priority Programme SPP1629 (grants SP 581/6-1 and SP 581/6-2 to C.S.; grant NE 648/5-2 to P.J.N.), and Collaborative Research Center SFB 824 (project C8) (C.S.), as well as the Wilhelm Sander-Stiftung (grant 2014.129.1 to C.S. and P.J.N.). This work was performed as partial fulfillment of the doctoral thesis of M.T. at the Faculty for Chemistry and Pharmacy of the LMU Munich.

REFERENCES

1. Repasky, E.A., Evans, S.S., and Dewhirst, M.W. (2013). Temperature matters! And why it should matter to tumor immunologists. Cancer Immunol. Res. *1*, 210–216.
2. Hildebrandt, B., Wust, P., Ahlers, O., Dieing, A., Sreenivasa, G., Kerner, T., Felix, R., and Riess, H. (2002). The cellular and molecular basis of hyperthermia. Crit. Rev. Oncol. Hematol. *43*, 33–56.
3. Ahmed, K., and Zaidi, S.F. (2013). Treating cancer with heat: hyperthermia as promising strategy to enhance apoptosis. J. Pak. Med. Assoc. *63*, 504–508.
4. Limmer, S., Hahn, J., Schmidt, R., Wachholz, K., Zengerle, A., Lechner, K., Eibl, H., Issels, R.D., Hossann, M., and Lindner, L.H. (2014). Gemcitabine treatment of rat soft tissue sarcoma with phosphatidyldiglycerol-based thermosensitive liposomes. Pharm. Res. *31*, 2276–2286.
5. Zimmermann, K., Hossann, M., Hirschberger, J., Troedson, K., Peller, M., Schneider, M., Brühschwein, A., Meyer-Lindenberg, A., Wess, G., Wergin, M., et al. (2017). A pilot trial of doxorubicin containing phosphatidyldiglycerol based thermosensitive liposomes in spontaneous feline soft tissue sarcoma. Int. J. Hyperthermia *33*, 178–190.
6. Frey, B., Weiss, E.M., Rubner, Y., Wunderlich, R., Ott, O.J., Sauer, R., Fietkau, R., and Gaipl, U.S. (2012). Old and new facts about hyperthermia-induced modulations of the immune system. Int. J. Hyperthermia *28*, 528–542.
7. Evans, S.S., Wang, W.C., Bain, M.D., Burd, R., Ostberg, J.R., and Repasky, E.A. (2001). Fever-range hyperthermia dynamically regulates lymphocyte delivery to high endothelial venules. Blood *97*, 2727–2733.
8. Skitzki, J.J., Repasky, E.A., and Evans, S.S. (2009). Hyperthermia as an immunotherapy strategy for cancer. Curr. Opin. Investig. Drugs *10*, 550–558.
9. De Becker, A., and Van Riet, I. (2016). Homing and migration of mesenchymal stromal cells: How to improve the efficacy of cell therapy? World J. Stem Cells *8*, 73–87.
10. Karp, J.M., and Leng Teo, G.S. (2009). Mesenchymal stem cell homing: the devil is in the details. Cell Stem Cell *4*, 206–216.
11. Conget, P.A., and Minguell, J.J. (1999). Phenotypical and functional properties of human bone marrow mesenchymal progenitor cells. J. Cell. Physiol. *181*, 67–73.
12. Kalimuthu, S., Zhu, L., Oh, J.M., Gangadaran, P., Lee, H.W., Baek, S.H., Rajendran, R.L., Gopal, A., Jeong, S.Y., Lee, S.W., et al. (2018). Migration of mesenchymal stem cells to tumor xenograft models and *in vitro* drug delivery by doxorubicin. Int. J. Med. Sci. *15*, 1051–1061.
13. Shi, S., Zhang, M., Guo, R., Miao, Y., and Li, B. (2019). Bone Marrow-Derived Mesenchymal Stem Cell-Mediated Dual-Gene Therapy for Glioblastoma. Hum. Gene Ther. *30*, 106–117.
14. Xu, S., Menu, E., De Becker, A., Van Camp, B., Vanderkerken, K., and Van Riet, I. (2012). Bone marrow-derived mesenchymal stromal cells are attracted by multiple myeloma cell-produced chemokine CCL25 and favor myeloma cell growth in vitro and in vivo. Stem Cells *30*, 266–279.
15. Kidd, S., Spaeth, E., Dembinski, J.L., Dietrich, M., Watson, K., Klopp, A., Battula, V.L., Weil, M., Andreeff, M., and Marini, F.C. (2009). Direct evidence of mesenchymal stem cell tropism for tumor and wounding microenvironments using in vivo bioluminescent imaging. Stem Cells *27*, 2614–2623.
16. Knoop, K., Schwenk, N., Schmohl, K., Müller, A., Zach, C., Cyran, C., Carlsen, J., Böning, G., Bartenstein, P., Göke, B., et al. (2015). Mesenchymal stem cell-mediated, tumor stroma-targeted radioiodine therapy of metastatic colon cancer using the sodium iodide symporter as theranostic gene. J. Nucl. Med. *56*, 600–606.
17. Bayo, J., Marrodán, M., Aquino, J.B., Silva, M., García, M.G., and Mazzolini, G. (2014). The therapeutic potential of bone marrow-derived mesenchymal stromal cells on hepatocellular carcinoma. Liver Int. *34*, 330–342.
18. Knoop, K., Kolokythas, M., Klutz, K., Willhauck, M.J., Wunderlich, N., Draganovici, D., Zach, C., Gildehaus, F.J., Böning, G., Göke, B., et al. (2011). Image-guided, tumor stroma-targeted 131I therapy of hepatocellular cancer after systemic mesenchymal stem cell-mediated NIS gene delivery. Mol. Ther. *19*, 1704–1713.
19. Penheiter, A.R., Wegman, T.R., Classic, K.L., Dingli, D., Bender, C.E., Russell, S.J., and Carlson, S.K. (2010). Sodium iodide symporter (NIS)-mediated radiovirotherapy for pancreatic cancer. AJR Am. J. Roentgenol. *195*, 341–349.
20. Schug, C., Gupta, A., Urnauer, S., Steiger, K., Cheung, P.F., Neander, C., Savvatakis, K., Schmohl, K.A., Trajkovic-Arsic, M., Schwenk, N., et al. (2019). A Novel Approach for Image-Guided ^{131}I Therapy of Pancreatic Ductal Adenocarcinoma Using Mesenchymal Stem Cell-Mediated NIS Gene Delivery. Mol. Cancer Res. *17*, 310–320.
21. Hall, B., Andreeff, M., and Marini, F. (2007). The participation of mesenchymal stem cells in tumor stroma formation and their application as targeted-gene delivery vehicles. Handb. Exp. Pharmacol. *2007*, 263–283.
22. Sun, Z., Wang, S., and Zhao, R.C. (2014). The roles of mesenchymal stem cells in tumor inflammatory microenvironment. J. Hematol. Oncol. *7*, 14.
23. Knoop, K., Schwenk, N., Dolp, P., Willhauck, M.J., Zischek, C., Zach, C., Hacker, M., Göke, B., Wagner, E., Nelson, P.J., and Spitzweg, C. (2013). Stromal targeting of sodium iodide symporter using mesenchymal stem cells allows enhanced imaging and therapy of hepatocellular carcinoma. Hum. Gene Ther. *24*, 306–316.
24. Müller, A.M., Schmohl, K.A., Knoop, K., Schug, C., Urnauer, S., Hagenhoff, A., Clevert, D.A., Ingrisch, M., Niess, H., Carlsen, J., et al. (2016). Hypoxia-targeted 131I therapy of hepatocellular cancer after systemic mesenchymal stem cell-mediated sodium iodide symporter gene delivery. Oncotarget *7*, 54795–54810.
25. Schug, C., Kitzberger, C., Sievert, W., Spellerberg, R., Tutter, M., Schmohl, K.A., Eberlein, B., Biedermann, T., Steiger, K., Zach, C., et al. (2019). Radiation-Induced Amplification of TGFB1-Induced Mesenchymal Stem Cell-Mediated Sodium Iodide Symporter (*NIS*) Gene ^{131}I Therapy. Clin. Cancer Res. *25*, 5997–6008.
26. Schug, C., Sievert, W., Urnauer, S., Müller, A.M., Schmohl, K.A., Wechselberger, A., Schwenk, N., Lauber, K., Schwaiger, M., Multhoff, G., et al. (2018). External Beam Radiation Therapy Enhances Mesenchymal Stem Cell-Mediated Sodium-Iodide Symporter Gene Delivery. Hum. Gene Ther. *29*, 1287–1300.
27. Schug, C., Urnauer, S., Jaeckel, C., Schmohl, K.A., Tutter, M., Steiger, K., Schwenk, N., Schwaiger, M., Wagner, E., Nelson, P.J., and Spitzweg, C. (2019). TGFB1-driven mesenchymal stem cell-mediated NIS gene transfer. Endocr. Relat. Cancer *26*, 89–101.

28. Tutter, M., Schug, C., Schmohl, K.A., Urnauer, S., Schwenk, N., Petrini, M., Lokerse, W.J.M., Zach, C., Ziegler, S., Bartenstein, P., et al. (2020). Effective control of tumor growth through spatial and temporal control of theranostic sodium iodide symporter (*NIS*) gene expression using a heat-inducible gene promoter in engineered mesenchymal stem cells. Theranostics *10*, 4490–4506.

29. Baril, P., Martin-Duque, P., and Vassaux, G. (2010). Visualization of gene expression in the live subject using the Na/I symporter as a reporter gene: applications in biotherapy. Br. J. Pharmacol. *159*, 761–771.

30. Penheiter, A.R., Russell, S.J., and Carlson, S.K. (2012). The sodium iodide symporter (NIS) as an imaging reporter for gene, viral, and cell-based therapies. Curr. Gene Ther. *12*, 33–47.

31. Ravera, S., Reyna-Neyra, A., Ferrandino, G., Amzel, L.M., and Carrasco, N. (2017). The Sodium/Iodide Symporter (NIS): Molecular Physiology and Preclinical and Clinical Applications. Annu. Rev. Physiol. *79*, 261–289.

32. Spitzweg, C., Bible, K.C., Hofbauer, L.C., and Morris, J.C. (2014). Advanced radioiodine-refractory differentiated thyroid cancer: the sodium iodide symporter and other emerging therapeutic targets. Lancet Diabetes Endocrinol. *2*, 830–842.

33. Spaeth, E., Klopp, A., Dembinski, J., Andreeff, M., and Marini, F. (2008). Inflammation and tumor microenvironments: defining the migratory itinerary of mesenchymal stem cells. Gene Ther. *15*, 730–738.

34. Ponte, A.L., Marais, E., Gallay, N., Langonné, A., Delorme, B., Hérault, O., Charbord, P., and Domenech, J. (2007). The in vitro migration capacity of human bone marrow mesenchymal stem cells: comparison of chemokine and growth factor chemotactic activities. Stem Cells *25*, 1737–1745.

35. Von Lüttichau, I., Notohamiprodjo, M., Wechselberger, A., Peters, C., Henger, A., Seliger, C., Djafarzadeh, R., Huss, R., and Nelson, P.J. (2005). Human adult CD34-progenitor cells functionally express the chemokine receptors CCR1, CCR4, CCR7, CXCR5, and CCR10 but not CXCR4. Stem Cells Dev. *14*, 329–336.

36. Hagenhoff, A., Bruns, C.J., Zhao, Y., von Lüttichau, I., Niess, H., Spitzweg, C., and Nelson, P.J. (2016). Harnessing mesenchymal stem cell homing as an anticancer therapy. Expert Opin. Biol. Ther. *16*, 1079–1092.

37. Rao, W., Deng, Z.S., and Liu, J. (2010). A review of hyperthermia combined with radiotherapy/chemotherapy on malignant tumors. Crit. Rev. Biomed. Eng. *38*, 101–116.

38. Issels, R., Kampmann, E., Kanaar, R., and Lindner, L.H. (2016). Hallmarks of hyperthermia in driving the future of clinical hyperthermia as targeted therapy: translation into clinical application. Int. J. Hyperthermia *32*, 89–95.

39. Toraya-Brown, S., and Fiering, S. (2014). Local tumour hyperthermia as immunotherapy for metastatic cancer. Int. J. Hyperthermia *30*, 531–539.

40. Dewhirst, M.W., Lee, C.T., and Ashcraft, K.A. (2016). The future of biology in driving the field of hyperthermia. Int. J. Hyperthermia *32*, 4–13.

41. Foster, D.S., Jones, R.E., Ransom, R.C., Longaker, M.T., and Norton, J.A. (2018). The evolving relationship of wound healing and tumor stroma. JCI Insight *3*, e99911.

42. von Einem, J.C., Guenther, C., Volk, H.D., Grütz, G., Hirsch, D., Salat, C., Stoetzer, O., Nelson, P.J., Michl, M., Modest, D.P., et al. (2019). Treatment of advanced gastrointestinal cancer with genetically modified autologous mesenchymal stem cells: Results from the phase 1/2 TREAT-ME-1 trial. Int. J. Cancer *145*, 1538–1546.

43. Rosová, I., Dao, M., Capoccia, B., Link, D., and Nolta, J.A. (2008). Hypoxic preconditioning results in increased motility and improved therapeutic potential of human mesenchymal stem cells. Stem Cells *26*, 2173–2182.

44. Egea, V., von Baumgarten, L., Schichor, C., Berninger, B., Popp, T., Neth, P., Goldbrunner, R., Kienast, Y., Winkler, F., Jochum, M., and Ries, C. (2011). TNF-α respecifies human mesenchymal stem cells to a neural fate and promotes migration toward experimental glioma. Cell Death Differ. *18*, 853–863.

45. Lourenco, S., Teixeira, V.H., Kalber, T., Jose, R.J., Floto, R.A., and Janes, S.M. (2015). Macrophage migration inhibitory factor-CXCR4 is the dominant chemotactic axis in human mesenchymal stem cell recruitment to tumors. J. Immunol. *194*, 3463–3474.

46. Shi, M., Li, J., Liao, L., Chen, B., Li, B., Chen, L., Jia, H., and Zhao, R.C. (2007). Regulation of CXCR4 expression in human mesenchymal stem cells by cytokine treatment: role in homing efficiency in NOD/SCID mice. Haematologica *92*, 897–904.

47. Droujinine, I.A., Eckert, M.A., and Zhao, W. (2013). To grab the stroma by the horns: from biology to cancer therapy with mesenchymal stem cells. Oncotarget *4*, 651–664.

48. Dwyer, R.M., Khan, S., Barry, F.P., O'Brien, T., and Kerin, M.J. (2010). Advances in mesenchymal stem cell-mediated gene therapy for cancer. Stem Cell Res. Ther. *1*, 25.

49. Baek, S.J., Kang, S.K., and Ra, J.C. (2011). In vitro migration capacity of human adipose tissue-derived mesenchymal stem cells reflects their expression of receptors for chemokines and growth factors. Exp. Mol. Med. *43*, 596–603.

50. Fajardo, L.F. (1984). Pathological effects of hyperthermia in normal tissues. Cancer Res. *44* (*Suppl 10*), 4826s–4835s.

51. Vaupel, P.W., and Kelleher, D.K. (2010). Pathophysiological and vascular characteristics of tumours and their importance for hyperthermia: heterogeneity is the key issue. Int. J. Hyperthermia *26*, 211–223.

52. Chen, J., Shi, Z.D., Ji, X., Morales, J., Zhang, J., Kaur, N., and Wang, S. (2013). Enhanced osteogenesis of human mesenchymal stem cells by periodic heat shock in self-assembling peptide hydrogel. Tissue Eng. Part A *19*, 716–728.

53. Alekseenko, L.L., Zemelko, V.I., Domnina, A.P., Lyublinskaya, O.G., Zenin, V.V., Pugovkina, N.A., Kozhukharova, I.V., Borodkina, A.V., Grinchuk, T.M., Fridlyanskaya, I.I., and Nikolsky, N.N. (2014). Sublethal heat shock induces premature senescence rather than apoptosis in human mesenchymal stem cells. Cell Stress Chaperones *19*, 355–366.

54. Rühle, A., Thomsen, A., Saffrich, R., Voglstätter, M., Bieber, B., Sprave, T., Wuchter, P., Vaupel, P., Huber, P.E., Grosu, A.L., and Nicolay, N.H. (2020). Multipotent mesenchymal stromal cells are sensitive to thermic stress—potential implications for therapeutic hyperthermia. Int. J. Hyperthermia *37*, 430–441.

55. Dwyer, R.M., Ryan, J., Havelin, R.J., Morris, J.C., Miller, B.W., Liu, Z., Flavin, R., O'Flatharta, C., Foley, M.J., Barrett, H.H., et al. (2011). Mesenchymal Stem Cell-mediated delivery of the sodium iodide symporter supports radionuclide imaging and treatment of breast cancer. Stem Cells *29*, 1149–1157.

56. Mansfield, D.C., Kyula, J.N., Rosenfelder, N., Chao-Chu, J., Kramer-Marek, G., Khan, A.A., Roulstone, V., McLaughlin, M., Melcher, A.A., Vile, R.G., et al. (2016). Oncolytic vaccinia virus as a vector for therapeutic sodium iodide symporter gene therapy in prostate cancer. Gene Ther. *23*, 357–368.

57. Trujillo, M.A., Oneal, M.J., McDonough, S., Qin, R., and Morris, J.C. (2012). A steep radioiodine dose response scalable to humans in sodium-iodide symporter (NIS)-mediated radiovirotherapy for prostate cancer. Cancer Gene Ther. *19*, 839–844.

58. Dingli, D., Peng, K.W., Harvey, M.E., Greipp, P.R., O'Connor, M.K., Cattaneo, R., Morris, J.C., and Russell, S.J. (2004). Image-guided radiovirotherapy for multiple myeloma using a recombinant measles virus expressing the thyroidal sodium iodide symporter. Blood *103*, 1641–1646.

59. Niess, H., Bao, Q., Conrad, C., Zischek, C., Notohamiprodjo, M., Schwab, F., Schwarz, B., Huss, R., Jauch, K.W., Nelson, P.J., and Bruns, C.J. (2011). Selective targeting of genetically engineered mesenchymal stem cells to tumor stroma microenvironments using tissue-specific suicide gene expression suppresses growth of hepatocellular carcinoma. Ann. Surg. *254*, 767–774, discussion 774–775.

60. Fischer, U.M., Harting, M.T., Jimenez, F., Monzon-Posadas, W.O., Xue, H., Savitz, S.I., Laine, G.A., and Cox, C.S., Jr. (2009). Pulmonary passage is a major obstacle for intravenous stem cell delivery: the pulmonary first-pass effect. Stem Cells Dev. *18*, 683–692.

61. Xie, C., Yang, Z., Suo, Y., Chen, Q., Wei, D., Weng, X., Gu, Z., and Wei, X. (2017). Systemically Infused Mesenchymal Stem Cells Show Different Homing Profiles in Healthy and Tumor Mouse Models. Stem Cells Transl. Med. *6*, 1120–1131.

62. Daldrup-Link, H.E., Rudelius, M., Metz, S., Piontek, G., Pichler, B., Settles, M., Heinzmann, U., Schlegel, J., Oostendorp, R.A., and Rummeny, E.J. (2004). Cell tracking with gadophrin-2: a bifunctional contrast agent for MR imaging, optical imaging, and fluorescence microscopy. Eur. J. Nucl. Med. Mol. Imaging *31*, 1312–1321.

63. Issels, R.D., Lindner, L.H., Verweij, J., Wessalowski, R., Reichardt, P., Wust, P., Ghadjar, P., Hohenberger, P., Angele, M., Salat, C., et al.; European Organization for the Research and Treatment of Cancer-Soft Tissue and Bone Sarcoma Group and the European Society for Hyperthermic Oncology (2018). Effect of Neoadjuvant Chemotherapy Plus Regional Hyperthermia on Long-term Outcomes Among Patients With Localized High-Risk Soft Tissue Sarcoma: The EORTC 62961-ESHO 95 Randomized Clinical Trial. JAMA Oncol. *4*, 483–492.

64. Thorén, F.B., Anderson, H., and Strannegård, Ö. (2013). Late divergence of survival curves in cancer immunotherapy trials: interpretation and implications. Cancer Immunol. Immunother. *62*, 1547–1551.

65. Wendtner, C.M., Abdel-Rahman, S., Krych, M., Baumert, J., Lindner, L.H., Baur, A., Hiddemann, W., and Issels, R.D. (2002). Response to neoadjuvant chemotherapy combined with regional hyperthermia predicts long-term survival for adult patients with retroperitoneal and visceral high-risk soft tissue sarcomas. J. Clin. Oncol. *20*, 3156–3164.

66. Datta, N.R., Ordóñez, S.G., Gaipl, U.S., Paulides, M.M., Crezee, H., Gellermann, J., Marder, D., Puric, E., and Bodis, S. (2015). Local hyperthermia combined with radiotherapy and-/or chemotherapy: recent advances and promises for the future. Cancer Treat. Rev. *41*, 742–753.

67. Spitzweg, C., Baker, C.H., Bergert, E.R., O'Connor, M.K., and Morris, J.C. (2007). Image-guided radioiodide therapy of medullary thyroid cancer after carcinoembryonic antigen promoter-targeted sodium iodide symporter gene expression. Hum. Gene Ther. *18*, 916–924.